



HAL
open science

Bis-Alkylureido Imidazole Artificial Water Channels

Dan-dan Su, Sébastien Ulrich, Mihail Barboiu

► **To cite this version:**

Dan-dan Su, Sébastien Ulrich, Mihail Barboiu. Bis-Alkylureido Imidazole Artificial Water Channels. *Angewandte Chemie International Edition*, 2023, 62 (35), pp.e2023062. 10.1002/anie.202306265 . hal-04188131

HAL Id: hal-04188131

<https://hal.umontpellier.fr/hal-04188131>

Submitted on 25 Oct 2023

HAL is a multi-disciplinary open access archive for the deposit and dissemination of scientific research documents, whether they are published or not. The documents may come from teaching and research institutions in France or abroad, or from public or private research centers.

L'archive ouverte pluridisciplinaire **HAL**, est destinée au dépôt et à la diffusion de documents scientifiques de niveau recherche, publiés ou non, émanant des établissements d'enseignement et de recherche français ou étrangers, des laboratoires publics ou privés.

Self-Assembly

Bis-Alkylureido Imidazole Artificial Water Channels

Dan-Dan Su, Sébastien Ulrich, and Mihail Barboiu*

Abstract: Nature creates aquaporins to effectively transport water, rejecting all ions including protons. Aquaporins (AQPs) has brought inspiration for the development of Artificial Water Channels (AWCs). Imidazole-quartet (I-quartet) was the first AWC that enabled to self-assemble a tubular backbone for rapid water and proton permeation with total ion rejection. Here, we report the discovery of bis-alkylureido imidazole compounds, which outperform the I-quartets by exhibiting ≈ 3 times higher net and single channel permeabilities (10^7 H₂O/s/channel) and a ≈ 2 – 3 times lower proton conductance. The higher water conductance regime is associated to the high partition of more hydrophobic bis-alkylureido channels in the membrane and to their pore sizes, experiencing larger fluctuations, leading to an increase in the number of water molecules in the channel, with decreasing H-bonding connectivity. This new class of AWCs will open new pathways toward scalable membranes with enhanced water transport performances.

Proteins channels are a class of biomolecules that span the cell membrane, enabling small polar solutes including water and ions to be transported through the hydrophobic membrane bilayer. Selective water or proton transport through proteins is essential for generating and using ion gradients in cells. Several proteins have been well-known to translocate water or proton,^[1,2] for instance aquaporins AQPs^[3,4] M2 channel^[2] and Gramicidin.^[5] Water and protons are translocated along H-bonded water wires. AQPs have two water-wires which antiparallel orientation lead to proton rejection.^[3] Differently, the gramicidin A with an uniform water orientation generates dipolar water-wire for proton translocation.^[5]

[*] D.-D. Su, Dr. M. Barboiu

 Institut Européen des Membrane, Adaptive Supramolecular Nano-
 systems Group, University of Montpellier, ENSCM, CNRS
 Place Eugène Bataillon, CC 047, 34095 Montpellier (France)
 E-mail: mihail-dumitru.barboiu@umontpellier.fr

D.-D. Su, S. Ulrich

 Institut des Biomolécules Max Mousseron (IBMM), Université de
 Montpellier, CNRS, ENSCM
 34090 Montpellier (France)

© 2023 The Authors. Angewandte Chemie International Edition published by Wiley-VCH GmbH. This is an open access article under the terms of the Creative Commons Attribution License, which permits use, distribution and reproduction in any medium, provided the original work is properly cited.

These discoveries have motivated researchers to design potential artificial channels to mimic natural proteins for scalable environmental applications, given that the barriers brought from the preparation of large-scale proteins-integrated membrane are hard to surmount.^[6,7] During the last decade, researchers have paid much attention in developing synthetic artificial water channels-AWCs including carbon nanotube porins,^[8] foldamers,^[9,10] pillararenes,^[11] I-quartets,^[12] hydroxy channels,^[13] or organic cages.^[14] Understanding and controlling the water transport mechanisms at the atom-level scale is extremely important. It relates to control specific water binding, self-assembly and biomimetic translocation toward the development of selective membranes for water desalination.

In our group, we have previously synthesized imidazole-quartet (I-quartet, **HCX**, Figure 1a) from histamine H and the corresponding alkyl-isocyanates CX and that form efficient AWCs in bilayer and polymeric membranes.^[15] Four imidazoles and two water molecules are H-bonded via imidazole-imidazole CH–N and imidazole-water N–H–O and NH–O–H H-bonds to form an Å-scale channel, that efficiently

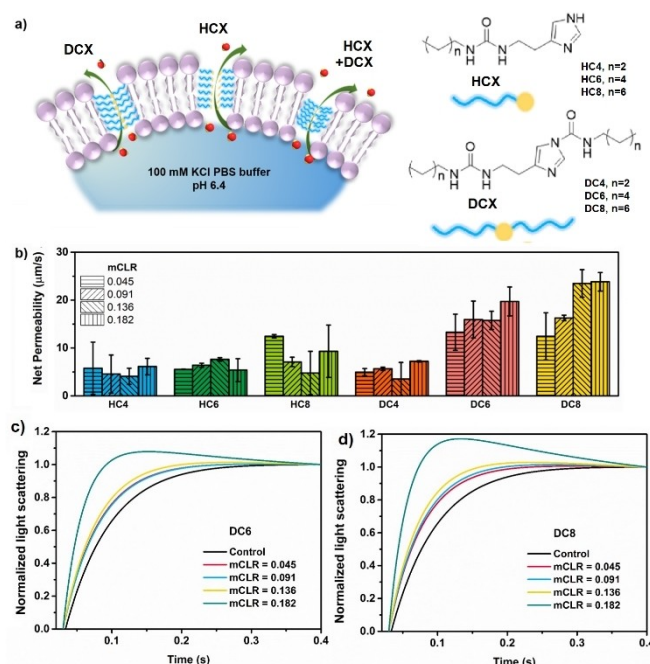


Figure 1. a) Chemical structures of mono-/bis-alkylureido imidazole **HCX/DCX** compounds (right) and the schematic representation of their assumed I-quartet/**DCX** channels within lipid bilayer (left); b) Water net permeability of **HCX** and **DCX** compounds at different mCLR (molar Compound to Lipid Ratio) in 100 mM KCl PBS buffer solution by exposing to hypertonic 300 mM KCl PBS buffer solution at pH 6.4; Normalized light scattering of c) **DC6** and d) **DC8**.

transport water and protons with a strong water-wire dipolar conservation.^[12] We serendipitously discovered that the addition to a small excess of alkyl-isocyanate to the reaction mixture led to the formation of doubly substituted Imidazole-N-CONH & -NHCONH bis-alkylureido imidazole compounds. The reaction of imidazole^[16a] or triazoles^[16b] and isocyanates is known to occur in anhydrous solvents, being sensitive to atmospheric moisture. In this context, we decided to optimize the synthesis of bis-alkylureido imidazoles **DCX** prepared from histamine and double alkyl chains, and found that they form very efficient channels displaying enhanced water transport with lower proton translocation compared to the previous mono-substituted alkylureido-imidazoles **HCX**. Two equivalents of butyl-, hexyl-, and octyl- isocyanates were added to a suspension of one equivalent of histamine in acetonitrile/ethyl acetate, to obtain the corresponding bis-alkylureido-imidazoles **DC4**, **DC6** and **DC8** (Figure 1a). ¹H and ¹³C NMR spectra in CDCl₃ and high-resolution mass spectra (ESI-MS+) confirm the chemical structure of **DC4**, **DC6** and **DC8** (Figures S1–S12). The **DCX**, were tested, compared and mixed with I-quartets for water, ion and proton transport.

We first investigated the water permeability of **DCX** channels and/or I-quartets by using standard stopped-flow technique.^[12b] Monodisperse unilamellar vesicles (average diameter ≈ 100 nm) were prepared using phosphatidylcholine lipid hydrated with 10 mM PBS buffer of 100 mM KCl osmolyte (pH = 6.4) (Figure 1a). The net permeabilities were determined after subtracting the controlled activity for membranes lacking channels. Each channel was tested at molar Compounds to Lipid Ratios (mCLRs) of **HCX** or **DCX** varying from 0.045 to 0.182. As shown in Figure 1b–d, **DCX** channels present an increased net water permeability, up to 20 μm/s for **DC6** and 25 μm/s for **DC8** at mCLR 0.182, compared to that of I-quartets ranging from 5 to 10 μm/s at the same dose (Table S1). We further estimated the single-channel permeability, P_s based on the following assumptions: i) spontaneous quantitative insertion of the **HCX** or **DCX** compounds into the lipid bilayer, supported by the observation of clear solutions at all concentrations used while turbidity is observed in absence of vesicles, and ii) the number of molecules needed to form a channel that spans the 5 nm bilayer is defined by the number of molecules that matches this distance in the crystal structure (in this case: 6 stacks/48 molecules).^[12] Accordingly, the single channel permeability values are 6.5×10^7 water/s/channel for **DC6** and 7.5×10^7 water/s/channel for **DC8** compared with 1.7×10^7 water/s/channel for **DC6** and 2.0×10^7 water/s/channel for **DC8**, which are on the same order of magnitude that of human aquaporin AQP0 (8.4×10^7 water/s/channel) and two orders of magnitude lower than AQP4 (8.0×10^9 water/s/channel)^[16b] (Table S2). Indeed, the hydrophobic **DC6-DC8** compounds are better partitioned in the membrane than **HC6-HC8** compounds, leading to higher water permeation when mixed with lipids. The tendency for increasing the net and single channel permeabilities at high concentration (most evident for **DC8** vs **HC8**, **DC6** vs **HC6**) can be explained not only by their higher partition in the membrane, but also by correlating, water molecular hydrogen bonding and its bond connectivity inside the pores. A low permeation regime accounting for rare

translocation events through **HC6-HC8** narrow channels has been previously identified as permutations between water molecules in an almost perfect single-file conformation.^[17] The higher permeation regimes associated to larger pore sizes of **DC6-DC8** are accompanied by the local breaking of the water single-file clusters with decreasing H-bond connectivity. This unique H-bonding behavior is related to an important morphology change of more permeable **DCX** channels presenting different self-assembly behaviors within the membrane. The lower associate strength of amide H-bond in **DCX** (**DC6-DC8**) compared the strong imidazole H-bond in I-quartet (**HC6-HC8**) leads to an increase in the number of less H-bonded water molecules in the channel, and therefore results in a three-fold increase of the single channel permeability.

We have then co-assembled an equimolar mixture of the **DCX/HCX** compounds. The net water permeability of the mixture present an average activity of the former components. Most probably, homomeric non-mixed **HC6&DC6** and **HC8&DC8** channels maintaining their own initial water permeability, led to median net permeabilities of ≈ 15 and 16.4 μm/s respectively corresponding to equal amount of individual channels separately operating within the bilayer membrane (Figure S13).

The HPTS (8-hydroxypyrene-1,3,6-trisulfonic acid trisodium salt) fluorescence assay was used to quantitatively estimate the proton/ion transport ability of **DCX** channels (Figure 2a).

A suspension of large unilamellar vesicles (LUVs) were formed using egg yolk L- α -phosphatidylcholine (EYPC) in 10 mM phosphate buffer solution with internal 100 mM KCl (pH 6.4) and external 100 mM MCl or 100 mM KX buffer ($M^+ = Na^+, Li^+, Cs^+, Rb^+, X^- = Br^-, I^-, NO_3^-, SO_4^{2-}$). The use of external Cl⁻ anions showed transport activity. Variation of cations and anions in the extravascular solution exhibited no considerable difference in ion transport rates, indicating that **DC4**, **DC6** and **DC8** do not transport most of the cations and anions (Figure S14). These activity profiles indicate the involvement of intravesicular Cl⁻ anions in the H⁺ symport, generating in the absence of valinomycin a variable efflux of protons (Figure 2 a, b). The H⁺ efflux activity is amplified in the presence of valinomycin (Val) K⁺ transporter via a supplementary electrogenic membrane polarization Val-K⁺ transport, indicating that dominant H⁺/Cl⁻ symport is supplemented by a H⁺/K⁺ antiport. The dose-response studies showed that the **DC6** is the most active one ($EC_{50} = 13.9$ μM and 11.7 μM in the absence and presence of valinomycin respectively), when compared with **DC8** ($EC_{50} = 19.4$ μM) and almost no activity for **DC4**. The Hill numbers are from 1 to 2, indicative of a low degree of cooperativity for the H⁺ transport. Unlike the **DCX** compounds, the dose response studies showed that the **HCX** compounds are not transporting H⁺ in the absence of valinomycin indicating that dominant H⁺/Cl⁻ symport is suppressed, most probably due to low binding of Cl⁻ by **HCX**, but showed a weak activity via Val-K⁺ electrogenic membrane polarization and H⁺/K⁺ antiport (Figure S15 and S16). To complete these experiments, we tested mixtures of the **DCX/HCX** compounds, leading to median H⁺ activities in the absence and in the presence of Val corresponding to equal amount of individual channels, as observed for

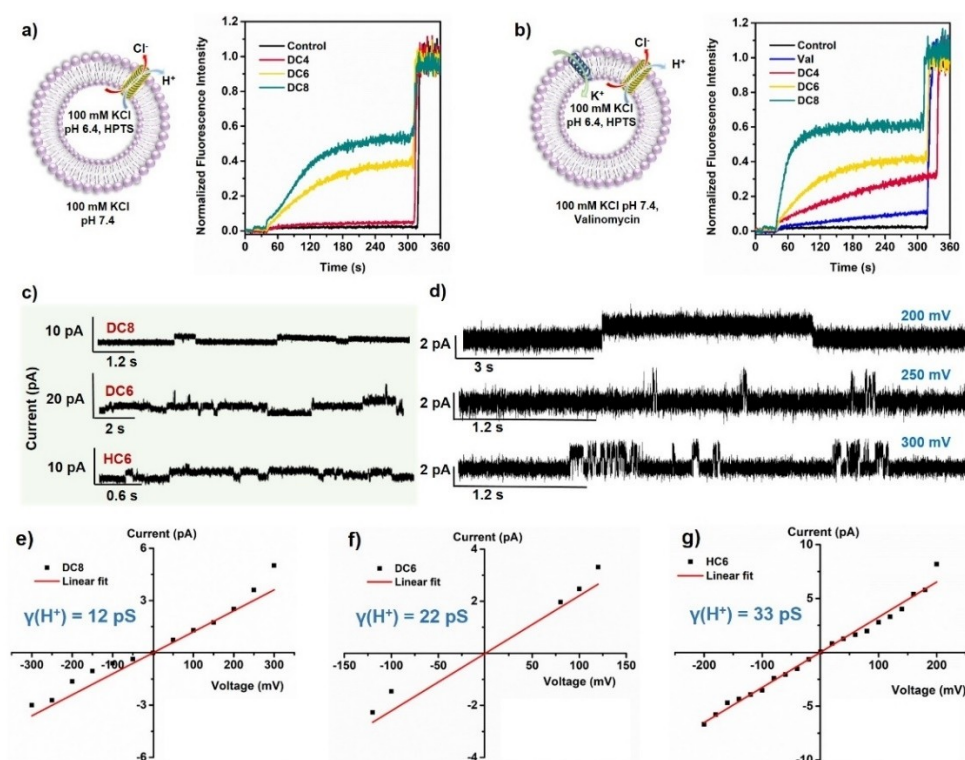


Figure 2. Normalized fluorescence intensity change as a function of time of **DC** channels a) in the absence or b) in the presence of valinomycin, internal composition: 100 mM KCl PBS buffer solution at pH 6.4; external composition: 100 mM KCl PBS buffer solution at pH 7.4; c) Representative single channel current traces for **DC8**, **DC6** and **HC6** recorded in symmetrical baths (*cis* chamber = *trans* chamber = 0.1 M HCl); d) The single channel current traces of cotransport **HC6&DC6** at varied voltages recorded in symmetrical baths (*cis* chamber = *trans* chamber = 0.1 M HCl); I-V plots of e) **DC8**, f) **DC6**, g) **HC6**.

water transport permeabilities through the bilayer membrane (Figure S17).

The proton transport activity of **DC/HC** compounds were evaluated by using patch-clamp technique using DOPC (1,2-dioleoyl-sn-glycero-3-phosphocholine, Avanti Polar lipids, 25 mg/mL in CHCl_3) in symmetrical solutions (*trans* = *cis* = 0.1 M HCl). As shown in Figure 2c, **DC8**, **DC6** and **HC6** exhibited long square channel signals, proving proton through the channels under electric stimuli. The slopes of the I-V plots showed that **DC8** has the lower proton conductance than **DC6** and **HC6** (Figures 2e–g, Figures S18–S20). The proton transport conductances **DC8** (12 pS) < **DC6** (22 pS) < **HC6** (33 pS) are following the opposite to the water transport performances. Unexpectedly, the co-assembly of **HC6&DC6** compounds led to low H^+ conductive hybrid channels ≈ 6 pS (Figure S21).

Assuming that all the compounds are inserted into the lipid bilayers, the H^+ flowing rates per nmol channel were determined by using the equation: $Q=It$, which the Q is the electric charge (C), I is the current flow (A) and t is the time interval (s), $1\text{ C}=1.6\times 10^{19}$ charges.^[18] It is assumed that **DC8** has the value of $\approx 2.4\times 10^5$ H^+ /s per nmol channel, and the higher flowing rates are calculated as $\approx 8.0\times 10^5$ H^+ /s per nmol channel, $\approx 12.3\times 10^5$ H^+ /s per nmol channel for **DC6** and **HC6** respectively, indicating that **DC8** has the lowest proton transport activity. The obvious rectangular traces show that indeed protons can permeate through the **HC6&DC6** channel mecha-

nism (Figure 2d), showing a strong *recessive* behavior with a H^+ flowing rate of $\approx 2.1\times 10^5$ H^+ /s per nmol channel which is significantly lower as observed for the former components.

We further investigated the selectivity of the H^+ over Cl^- transport of the **DC** channels, performing the planar lipid bilayer experiments in unsymmetrical solutions (*trans* chamber = 0.1 M HCl, *cis* chamber = 0.25 M HCl). The I-V curves and Goldman-Hodgkin-Katz analysis revealed a favorable H^+/Cl^- selectivity for **DC8** ($P_{\text{H}^+}/P_{\text{Cl}^-}=1.8$) and **DC6** ($P_{\text{H}^+}/P_{\text{Cl}^-}=1.7$) (Figure S22, S23), which are consistent with the HPTS fluorescence results revealing a rate-limiting barrier for the transport of Cl^- anions.

In conclusion, we discovered by serendipity a novel class of outstanding artificial water channels—**DCX** channels—which are based on bis-alkylureido imidazole compounds. These **DCX** compounds have increased lipophilicity and partition within membrane, and display increased water transport activities (three-fold better than the parent I-quartet) and lower H^+ translocation across lipid bilayer.

During H^+ translocation, the dipolar orientation of the water must be preserved and strongly favored by continuous H-bonding of water wires within channels. The structural heterogeneity within **DCX** channels induces an increase of the water mobility and most probably flickering discontinuous water wires that conduct protons less effectively than continuous dipolar water wires of I-quartet *via* Grothuss translocation.^[12a] Segmental heterogeneity due to the supple-

mentary alkylureido arms within **DC6** and **DC8** compounds, induce weak H-bonding among water molecules and most probably lead to the breakage of dipole conservation affecting the proton tunneling along channels. This was differently, observed with I-quartets where the dipolar orientation of continuous water wires is preserved and determined the steady proton translocation.^[15a] Our work highlights novel design strategies for the development of novel, more performant water transporting channels with less proton-conductive behaviors. We showed that close positioning of a supplementary alkylurea arms proximal to imidazole water binding sites resulted in channels that are highly selective for water, and conduct selectively protons with a H⁺/Cl⁻ selectivity. Our studies shed light on important information on potential mechanisms of biological proton/water translocation and shall inspire novel designs for engineering artificial water channels membranes.

Acknowledgements

D.-D. Su appreciates receiving a scholarship from China Scholarship Council as support at University of Montpellier, France. This work was supported by Agence Nationale de la Recherche ANR-22-CE06-0024-02, BIOWATER.

Conflict of Interest

The authors declare no conflict of interest.

Data Availability Statement

The data that support the findings of this study are available from the corresponding author upon reasonable request.

Keywords: Artificial Water Channels · Biomimetic · Hydrogen Bonding · Proton Transport · Self-Assembly

- [1] a) P. Agre, *Proc. Am. Thorac. Soc.* **2006**, *3*, 5–13; b) B. Yang, A. S. Verkman, *J. Biol. Chem.* **1997**, *272*, 16140–16146.
 [2] S. Phongphanphane, T. Rungrotmongkol, N. Yoshida, S. Hannongbua, F. Hirata, *J. Am. Chem. Soc.* **2010**, *132*, 9782–9788.
 [3] E. Tajkhorshid, P. Nollert, M. Jensen, L. J. W. Miercke, J. O’Connell, R. M. Stroud, K. Schulten, *Science* **2002**, *296*, 525–530.
 [4] A. Adeoye, A. Odugbemi, T. Ajewole, *Biointerface Res. Appl. Chem.* **2021**, *12*, 690–705.
 [5] R. Pomès, B. Roux, *Biophys. J.* **1996**, *71*, 19–39.
 [6] E. Abaie, L. Xu, Y.-X. Shen, *Front. Environ. Sci. Eng.* **2021**, *15*, 124.
 [7] a) D.-D. Su, M. Barboiu, *CCS Chem.* **2023**, *5*, 279–291; b) L.-B. Huang, M. Di Vincenzo, Y. Li, M. Barboiu, *Chem. Eur. J.* **2021**, *27*, 2224–2239.
 [8] a) R. H. Tunuguntla, R. Y. Henley, Y.-C. Yao, T. A. Pham, M. Wanunu, A. Noy, *Science* **2017**, *357*, 792–796; b) Y. Li, Z. Li, F.

- Aydin, J. Quan, X. Chen, Y.-C. Yao, C. Zhan, Y. Chen, T. A. Pham, A. Noy, *Sci. Adv.* **2020**, *6*, eaba9966 ; c) G. Hummer, J. C. Rasaiah, J. P. Noworyta, *Nature* **2001**, *414*, 188–190; d) Y. Hou, M. Wang, X. Chen, X. Hou, *Nano Res.* **2021**, *14*, 2171–2178.
 [9] a) J. Shen, R. Ye, A. Romanies, A. Roy, F. Chen, C. Ren, Z. Liu, H. Zeng, *J. Am. Chem. Soc.* **2020**, *142*, 10050–10058; b) A. Roy, J. Shen, H. Joshi, W. Song, Y.-M. Tu, R. Chowdhury, R. Ye, N. Li, C. Ren, M. Kumar, et al., *Nat. Nanotechnol.* **2021**, *16*, 911–917.
 [10] J. Shen, J. Fan, R. Ye, N. Li, Y. Mu, H. Zeng, *Angew. Chem. Int. Ed.* **2020**, *59*, 13328–13334.
 [11] a) Z.-J. Yan, D. Wang, Z. Ye, T. Fan, G. Wu, L. Deng, L. Yang, B. Li, J. Liu, T. Ma, et al., *J. Am. Chem. Soc.* **2020**, *142*, 15638–15643; b) D. Strilets, S. Fa, A. Hardiagon, M. Baaden, T. Ogoshi, M. Barboiu, *Angew. Chem. Int. Ed.* **2020**, *59*, 23213–23219; c) W. Song, H. Joshi, R. Chowdhury, J. S. Najem, Y.-X. Shen, C. Lang, C. B. Henderson, Y.-M. Tu, M. Farrell, M. E. Pitz, et al., *Nat. Nanotechnol.* **2020**, *15*, 73–79; d) X.-B. Hu, Z. Chen, G. Tang, J.-L. Hou, Z.-T. Li, *J. Am. Chem. Soc.* **2012**, *134*, 8384–8387; e) Q. Xiao, T. Fan, Y. Wang, Z.-T. Li, J.-L. Hou, Y. Wang, *CCS Chem.* **2023**, <https://doi.org/10.31635/ccschem.023.202302975>.
 [12] a) Y. Le Duc, M. Michau, A. Gilles, V. Gence, Y.-M. Legrand, A. van der Lee, S. Tingry, M. Barboiu, *Angew. Chem. Int. Ed.* **2011**, *50*, 11366–11372; b) E. Licsandru, I. Kocsis, Y.-X. Shen, S. Murail, Y.-M. Legrand, A. van der Lee, D. Tsai, M. Baaden, M. Kumar, M. Barboiu, *J. Am. Chem. Soc.* **2016**, *138*, 5403–5409; c) L.-B. Huang, M. Di Vincenzo, M. G. Ahunbay, A. van der Lee, D. Cot, S. Cerneaux, G. Maurin, M. Barboiu, *J. Am. Chem. Soc.* **2021**, *143*, 14386–14393.
 [13] a) L.-B. Huang, A. Hardiagon, I. Kocsis, C.-A. Jegu, M. Deleanu, A. Gilles, A. van der Lee, F. Sterpone, M. Baaden, M. Barboiu, *J. Am. Chem. Soc.* **2021**, *143*, 4224–4233; b) D. Mondal, B. R. Dandekar, M. Ahmad, A. Mondal, J. Mondal, P. Talukdar, *Chem. Sci.* **2022**, *13*, 9614–9623.
 [14] a) Y.-D. Yuan, J. Dong, J. Liu, D. Zhao, H. Wu, W. Zhou, H. X. Gan, Y. W. Tong, J. Jiang, D. Zhao, *Nat. Commun.* **2020**, *11*, 4927; b) X. Zhou, G. Liu, K. Yamato, Y. Shen, R. Cheng, X. Wei, W. Bai, Y. Gao, H. Li, Y. Liu, et al., *Nat. Commun.* **2012**, *3*, 949; c) H.-Y. Chang, K.-Y. Wu, W.-C. Chen, J.-T. Weng, C.-Y. Chen, A. Raj, H.-O. Hamaguchi, W.-T. Chuang, X. Wang, C.-L. Wang, *ACS Nano* **2021**, *15*, 14885–14890.
 [15] a) I. Kocsis, M. Sorci, H. Vanselous, S. Murail, S. E. Sanders, E. Licsandru, Y. M. Legrand, A. van der Lee, M. Baaden, P. B. Petersen, G. Belfort, M. Barboiu, *Sci. Adv.* **2018**, *4*, eaao5603; b) I. Kocsis, Z. Sun, Y. M. Legrand, M. Barboiu, *npj Clean Water* **2018**, *1*, 13.
 [16] a) K. J. Padiya, S. Gavade, B. Kardile, M. Tiwari, S. Bajare, M. Mane, V. Gaware, S. Varghese, D. Harel, Y. Se. Kurhade, *Org. Lett.* **2012**, *14*, 2814–2817; b) M. Barboiu, Y. Le Duc, A. Gilles, P.-A. Cazade, M. Michau, Y.-M. Legrand, A. van der Lee, B. Coasne, P. Parvizi, J. Post, T. Fyles, *Nat. Commun.* **2014**, *5*, 4142.
 [17] A. Hardiagon, S. Murail, L.-B. Huang, A. van der Lee, F. Sterpone, M. Barboiu, M. Baaden, *J. Chem. Phys.* **2021**, *154*, 184102.
 [18] T. Yan, S. Liu, J. Xu, H. Sun, S. Yu, J. Liu, *Nano Lett.* **2021**, *21*, 10462–10468.

Manuscript received: May 4, 2023

Accepted manuscript online: July 12, 2023

Version of record online: July 12, 2023